HHS Public Access

Author manuscript

Neuron. Author manuscript; available in PMC 2017 January 06.

Published in final edited form as:

Neuron. 2016 January 6; 89(1): 221–234. doi:10.1016/j.neuron.2015.11.028.

Relationships between pupil diameter and neuronal activity in the locus coeruleus, colliculi, and cingulate cortex

Siddhartha Joshi[1], **Yin Li**[1], **Rishi Kalwani**[2], and **Joshua I. Gold**[1]

[1] Department of Neuroscience, University of Pennsylvania, Philadelphia, PA 19104

[2] Temple University School of Medicine, Philadelphia, PA 19140

SUMMARY

Changes in pupil diameter that reflect effort and other cognitive factors are often interpreted in terms of the activity of norepinephrine-containing neurons in the brainstem nucleus locus coeruleus (LC), but there is little direct evidence for such a relationship. Here we show that LC activation reliably anticipates changes in pupil diameter that either fluctuate naturally or are driven by external events during near fixation, as in many psychophysical tasks. This relationship occurs on as fine a temporal and spatial scale as single spikes from single units. However, this relationship is not specific to the LC. Similar relationships, albeit with delayed timing and different reliabilities across sites, are evident in the inferior and superior colliculus and anterior and posterior cingulate cortex. Because these regions are interconnected with the LC, the results suggest that non-luminance-mediated changes in pupil diameter might reflect LC-mediated coordination of neuronal activity throughout some parts of the brain.

INTRODUCTION

Non-luminance-mediated changes in pupil diameter have long been used as markers of arousal and cognitive effort and more recently have been interpreted in terms of the explore-exploit trade-off, surprise, salience, decision biases, and other factors that can influence ongoing information processing (Jepma and Nieuwenhuis, 2011; Gilzenrat et al., 2010; Krugman, 1964; Granholm and Steinhauer, 2004; Schmidt and Fortin, 1982; Kahneman and Beatty, 1966; Richer and Beatty, 1987; Einhäuser et al., 2008; Alnæs et al., 2014; de Gee et al., 2014; Wang et al., 2014; Lavín et al., 2014; Eldar et al., 2013; Nassar et al., 2012; Takeuchi et al., 2011; Preuschoff et al., 2011; Einhäuser et al., 2010; McGinley et al., 2015). In many cases, these effects have been interpreted in terms of activation of norepinephrine (NE)-containing neurons in the brainstem nucleus locus coeruleus (LC). The proposed functional association between LC activation and pupil diameter is based largely on indirect

CONTACT: Siddhartha Joshi <sidjoshi@mail.med.upenn.edu>.

AUTHOR CONTRIBUTIONS

R.K. implemented the experimental task; S.J., Y.L., and R.K. collected the data; and S.J. and J.I.G. analyzed the data and wrote the paper. All authors designed the research; discussed the analyses, results, and interpretation; and revised the paper.

evidence, including anatomical and pharmacological studies, fMRI and EEG studies that measured both brain activity and pupil diameter, and common factors that drive LC and pupil changes (Phillips et al., 2000; Hou et al., 2005; Beatty, 1982b; Beatty, 1982a; Richer and Beatty, 1987; Einhäuser et al., 2008; Gilzenrat et al., 2010; Morad et al., 2000; Aston-Jones and Cohen, 2005; Murphy et al., 2011; Murphy et al., 2014). More direct evidence includes one commonly cited single-unit example (Aston-Jones and Cohen, 2005) and a recent report relating event-driven changes in LC spiking activity and pupil diameter in monkeys (Varazzani et al., 2015). Pupil diameter also can co-vary with neuronal activity in cortex, which is thought to reflect, at least in part, modulation by the LC-NE system (Vinck et al., 2015; Reimer et al., 2014; Ebitz and Platt, 2015; Eldar et al., 2013; McGinley et al., 2015). The goal of our study was to provide for the first time a direct and systematic examination of the timescale, magnitude, and prevalence of relationships between both spontaneous and event-driven changes in pupil diameter and neural activity in the LC and elsewhere in the brain.

We simultaneously measured pupil diameter and neural activity in several brain regions (recorded separately; Fig. 1) of alert, fixating monkeys, either during passive viewing or in response to arousing sounds. We targeted the LC and adjacent NE-containing subcoeruleus, which together we refer to as LC+ (Kalwani et al., 2014), plus several other brain regions interconnected with the LC-NE system. The inferior colliculus (IC) receives dense projections from LC and, as part of the ascending auditory pathway, is sensitive to our sound manipulation (Klepper and Herbert, 1991; Hormigo et al., 2012; Foote et al., 1983; Levitt and Moore, 1978). The intermediate layer of superior colliculus (SCi) also receives LC innervation and has been shown to contribute to the effects of contrast-based saliency on pupil dilation (Wang et al., 2014; Wang et al., 2012; Edwards et al., 1979). The anterior cingulate cortex (ACC) is a primary source of cortical input to the LC, receives projections from the LC, and has neural activity that encodes conflict-and surprise-related signals that can also be reflected in pupil diameter (Aston-Jones and Cohen, 2005; Ebitz and Platt, 2015; Porrino and Goldman-Rakic, 1982; Hayden et al., 2011). The posterior cingulate cortex (CGp) is strongly interconnected with the ACC and receives LC input (Levitt and Moore, 1978; Heilbronner and Haber, 2014).

We assessed relationships between pupil diameter and neural activity from each brain region in several ways. First, we directly compared pupil diameter and single-unit spiking activity during passive fixation, which allowed us to identify relationships that were not dependent on external events that might separately affect pupil diameter and neural activity. We assessed these relationships on different timescales, including sustained or baseline periods lasting several seconds and shorter periods that could be related to the timing of single spikes. Second, we analyzed pupil-related differences in local field potentials (LFPs), which can reflect neuromodulatory influences like that provided by the LC-NE system (Bari and Aston-Jones, 2013; Lee and Dan, 2012). Third, we tested whether changes in pupil diameter and in spiking activity evoked by repeated presentations of the same arousing sound stimulus at unpredictable times covary on a trial-by-trial basis (i.e., a test of noise correlations), to complement and extend recent findings that different task conditions can, on average, drive co-variations in pupil diameter and LC activity (i.e., a measure of signal correlations) (Varazzani et al., 2015). Fourth, for LC+, IC, and SCi, we used electrical

microstimulation to probe how reliably pupil changes can be elicited by manipulating local neural activity. The results indicate that pupil diameter can be a reliable marker of activation of LC+, but that this relationship is not specific to the LC+. Pupil diameter and neural activity are also reliably linked in the IC, SCi, and, to a lesser extent, cingulate cortex, possibly reflecting widespread, coordinating influences of the LC-NE system.

RESULTS

We related pupil diameter to neural activity measured separately in each of five brain regions (LC+: *n*=43 single units isolated from 33 multi-unit/LFP recording sites in monkey Oz and 61/52 in Ci; IC: 64/68 in Oz and 66/78 in Ci; plus smaller sample sizes for the remaining three regions, which can affect the reliability of the results: SCi: 14/12 in Oz and 21/20 sites in Ci; ACC: 40/43 in Sp and 6/7 in At; CGp: 25/13 in Sp and 10/14 in Ch; Fig. 1) while they maintained steady fixation (60 cm viewing distance) under dim, steady lighting conditions (luminance at the monkeys' eyes: 3.5 cd/m^2; luminance of the fixation spot measured on the display: 125 cd/m^2).

During stable, near fixation, pupil diameter tended to vary both across and within trials (Fig. 2A, B). In our monkeys, these pupil fluctuations were quasi-periodic, with oscillations at ~1–3 Hz evident on individual trials but with a periodicity and amplitude that varied considerably from cycle to cycle (Fig. 2B). We therefore characterized each cycle individually, in terms of the duration and magnitude of dilations and constrictions defined by zero-crossings of the first derivative of pupil diameter. These durations were broadly distributed <~1000 ms, with slightly longer dilations (overall median [interquartile range, or IQR] = 329 [230–471] ms) than constrictions (288 [211–395] ms; Wilcoxon rank-sum test, $p<0.01$) that were roughly consistent across the five monkeys (median dilations lasted between 290–351 ms and median constrictions lasted between 254–319 ms for each of the five monkeys; Fig. 2C). The magnitude of these fluctuations depended on the baseline value of pupil diameter at the time of the fluctuation, likely reflecting asymmetries in the mechanical properties of the iris musculature (Loewenfeld and Newsome, 1971): larger transient dilations occurred when the pupil was more constricted, and, to a lesser extent, larger transient constrictions occurred when the pupil was more dilated (Fig. 2D). These fluctuations were not consistently associated with small eye movements (Martinez-Conde et al., 2013; Krekelberg, 2011), which occurred less frequently and without a consistent phase relationship with respect to the fluctuations in pupil diameter (Fig. 2E). The pupil fluctuations also did not appear to reflect the monkeys' heart rate, which was typically the range of ~140–150 beats/min (i.e., a full period of ~400–430 ms, which was substantially shorter than the median full period of pupil fluctuations). Thus, these fluctuations appear to be consistent with previous reports of pupil noise (Stanten and Stark, 1966), spontaneous pupil oscillations (Warga et al., 2009), or pupillary unrest (Loewenfeld, 1999; Bokoch et al., 2015). These phenomena are not caused by similar microfluctuations in accommodation that can also occur during near fixation (Alpern et al., 1961; Stark and Atchison, 1997; Hunter et al., 2000) but instead are thought to reflect variability in the firing patterns of brainstem neurons that control pupil diameter (Loewenfeld, 1999; Bokoch et al., 2015).

Relationship between pupil diameter and spiking activity during passive fixation

During passive fixation, spontaneous fluctuations in pupil diameter had consistent relationships to concurrently measured spiking activity on relatively long (trial-by-trial) and short (with respect to individual spikes) timescales. As detailed below, these relationships were particularly strong for activity measured in LC+ and IC but were also evident for certain sites in SCi, ACC, and CGp.

As has been reported previously for one LC site (Aston-Jones and Cohen, 2005), we found numerous compelling examples of correlations between trial-by-trial average values of pupil diameter and spiking activity from select sites in several brain regions. An example LC+ session is shown in Fig. 3A–C. Trials with relatively dilated (constricted) pupils tended to correspond to relatively high (low) mean spike rates, even after accounting for overall linear trends of both measurements over the course of the session (partial Spearman's correlation coefficient = 0.45, $p<0.001$). Similar examples are shown for IC, ACC, and CGp (Fig. 3A–C). We also found some sites with negative correlations between pupil diameter and spike rate, particularly in SCi (an example session is shown in Fig. 3A–C).

These trial-by-trial relationships between pupil diameter and spike rates were statistically reliable across the populations of units we recorded in LC+ and IC but not SCi, ACC, or CGp. For LC+ and IC, the median correlation coefficient across individual units for each monkey was >0 (Wilcoxon rank-sum test, $p<0.004$ in all four cases) and did not differ for the two brain regions ($p>0.05$ for each monkey). Moreover, similar proportions of individual units from these regions showed significant, positive correlations (Fig. 3D). ACC units also had a tendency for such positive effects, but the median correlation coefficient was significantly >0 ($p<0.05$) for only one monkey. For SCi and CGp, the effects were smaller and more mixed, with more negative effects in SCi (Fig. 3D).

We found more reliable relationships between pupil diameter and neuronal activity from all five brain regions by analyzing these relationships on finer timescales. Figure 4 shows analyses of spike-triggered changes in pupil diameter; that is, the extent to which individual spikes were aligned in time with the first derivative of pupil diameter as a function of time. An example LC+ unit is shown in Fig. 4A. For this unit, spikes occurring during fixation tended to be followed immediately by a brief dilation, with the peak positive change in pupil diameter occurring 310 ms after the spike, then constriction, with the peak negative change in pupil diameter occurring 750 ms after the spike. These positive and negative peaks were both distinguishable from random relationships between the measured spikes and pupil data obtained at different times (i.e., by shuffling the trial-by-trial spike and pupil data relative to each other; gray lines in Fig. 4A). We found compelling examples of spike-triggered pupil effects from all five brain regions, each of which included a reliable dilation and then constriction occurring, on average, around or following the time of each spike (Fig. 4A).

Subsets of neurons recorded from each brain region and each monkey showed these kinds of reliable relationships between individual spikes and changes in pupil diameter. Population average spike-triggered changes in pupil diameter from each brain region are shown in Fig. 4B, and data from all recorded units, separated by monkey, are shown in Fig. 4C. These plots indicate qualitatively similar patterns of effects across many sites, particularly those in

LC+, IC, and SCi, with transient dilations and then constrictions following spikes. More quantitatively, 47–83% of sites in a given brain region and monkey showed statistically reliable differences between real and shuffled spike-triggered changes in pupil diameter (Fig. 4C). These differences occurred in relatively restricted time windows around the time of the spike. The magnitudes of these peak values, reflecting average maximal changes in pupil diameter around the time of each spike, did not covary with the magnitudes of trial-by-trial correlations between pupil diameter and spiking activity, reflecting the relationship between average pupil diameter and average spike rate over several seconds (see Fig. 3), from the same recording sites (H_0: Spearman's correlation coefficient=0, $p>0.05$ for each monkey and brain region). This result implies that pupil-spike relationships can take different forms over different timescales.

In addition to these rough similarities, there were differences in the timing of spike-triggered changes in pupil diameter across the five brain regions. The timing of the peaks of these curves, computed per brain region and per monkey, are shown for the population average traces in Fig. 4B and computed from individual sessions with reliable peaks for each monkey in Fig. 4C. In both cases, there was a progression of the peak times for data obtained across sites in the same monkeys (LC+, IC, and SCi), with the longest lag between the spike and the dilation-related peak occurring in LC+, then a delay to IC and finally SCi (an ANOVA with monkey and these three brain regions as factors had a main effect of brain region, $p=0.03$). The effects in cortex, measured in separate monkeys and thus not necessarily directly comparable to the subcortical results, did not, on average, have such clear peaks, reflecting less-consistent timing across recording sites even in the same brain region of a given monkey (Fig. 4B,C).

Complementary to these features of spike-triggered pupil measurements, there were notable patterns of pupil-triggered spike rates from all five brain regions (Fig. 5). We calculated peri-event time histograms (PETHs) relative to pupil dilation or constriction events (i.e., the times of the maximum increase or decrease in pupil diameter, respectively, as a function of time for each quasi-periodic half-cycle, as shown in Fig. 2B). Example units from all five brain regions showed similar pupil-dependent patterns in the rasters and associated PETHs: a transient increase in spiking preceding large dilation events (dark lines in Fig. 5B) and either little change or a transient decrease in spiking preceding large constriction events (light lines).

To visualize and quantify these effects, we computed for each single unit the mean difference in pupil-event-aligned spiking activity for large dilations versus large constrictions, as in the examples in Fig. 5A,B. Thus, positive (negative) values of this difference indicate higher (lower) spike rates in the given time bin relative to dilations versus constrictions. Population averages from each brain region are shown in Fig. 5C, and data from individual recording sites, separated by monkey, are shown in Fig 5D. The biggest and most consistent pupil-related modulations were evident in LC+ and IC. In these regions, a peak, positive modulation occurred, on average, in a relatively restricted time frame just prior to the pupil event. The timing of this peak progressed systematically across the brainstem sites, from LC+ to IC to SCi, relative to the pupil event (Fig. 5C,D). For the cortical sites, similar proportions of units as for the subcortical sites showed these

modulations (30–60%), but partly because the timing of these modulations varied considerably across units, the average effects were smaller in ACC and CGp (Fig. 5C,D).

Relationship between pupil diameter and LFPs during passive fixation

LFPs can represent different aspects of neuromodulatory influence and network function than spiking activity (Bari and Aston-Jones, 2013; Lee and Dan, 2012). We therefore also assessed relationships between spontaneous fluctuations in pupil diameter measured during passive fixation and LFPs. Pupil-linked effects were evident in the difference between dilation- and constriction-linked raw LFPs aligned to the time of pupil events. Example sites from each brain region showed a prominent negative trough preceding the pupil event, corresponding to more a more negative LFP value preceding dilations versus constrictions (Fig. 6A). This negative peak preceding the pupil event was evident in the population average traces, particularly for the brainstem sites (Fig. 6B), and many traces from individual sites from each brain region (Fig. 6C). Like for the spike-pupil analyses, the timing of this peak varied systematically across the brainstem sites, occurring earliest in LC +, then IC, then SCi. Across monkeys, the brainstem sites showed larger proportions of neurons with reliable effects (63%–100%) compared with cortical sites (14%–61%).

Because different frequency bands of the LFP can reflect different aspects of network function (von Stein and Sarnthein, 2000; Kopell et al., 2000; Donner and Siegel, 2011), we also assessed band-specific differences relative to pupil events (dilation versus constriction). We found prominent effects in LFP power in both low (<30Hz) and gamma (30–100Hz) frequency bands that differed for the different brain regions tested (Fig. 6D). For the brainstem sites, the peak effects occurred, on average, <500 ms before the associated pupil event, but primarily for the gamma band in LC+, both bands in IC, and the low-frequency band in SCi. For the cortical sites, the effects were more mixed, with both ACC and CGp showing some early enhancement in the gamma band but little pupil-dependent structure just prior to the pupil events.

Relationship between pupil diameter and neural activity in response to startling events

To examine the relationship between pupil diameter and neural activity in the context of not just internal (spontaneous) fluctuations but also external events that can cause changes in arousal, we played a brief, loud, startling tone during randomly chosen trials. For all monkeys, the tone caused a transient dilation of the pupil (Fig. 7A). We found that areas LC +, IC, and ACC also exhibited consistent, transient neuronal responses to the tone in each of two monkeys (Fig. 7B). In contrast, the tone evoked consistent responses in the CGp of only one of two monkeys and did not evoke consistent responses in the SCi of either of two monkeys (Fig. 7B). On a trial-by-trial basis, there was a weak but reliable relationship between the magnitudes of the tone-aligned neural and pupil responses only for LC+, consistent with a common driving input that has more direct effects on LC+ than the other brain regions tested (Nieuwenhuis et al., 2011) (Fig. 7C).

Relationship between pupil diameter and electrical microstimulation

We used electrical microstimulation to test if manipulation of neuronal activity at a given site in the LC+, IC, or SCi could evoke changes pupil diameter. We found sites in each of

these brain regions where microstimulation reliably evoked transient increases in pupil diameter within ~1000 ms of microstimulation onset (Fig. 8A). Across the population of tested sites, the effects were most consistent in LC+ (Fig. 8B). There, microstimulation evoked changes in pupil diameter at all tested sites (n=12), and across sites the time of the maximum evoked change in pupil diameter had mean values (per site) of 458–563 ms following microstimulation onset. In IC, the effects were slightly more variable. There, microstimulation evoked changes in pupil diameter at 12 out of 18 sites, and the time of the maximum change was 253–653 ms following microstimulation onset. Microstimulation in SCi yielded reliable changes in pupil diameter from 3 of 10 tested sites, as has been reported previously (Wang et al., 2012). The timing of these effects were more variable than for LC+ or IC, with the time of the maximum change occurring 388–813 ms following microstimulation onset.

DISCUSSION

The goal of this study was to characterize relationships between non-luminance-mediated changes in pupil diameter and neural activity. We targeted the LC (plus the adjacent subcoeruleus, which is difficult to distinguish from the LC using our recording techniques (Kalwani et al., 2014)) because of its previously proposed links to pupil diameter (Nassar et al., 2012; Nieuwenhuis et al., 2011; Varazzani et al., 2015; Phillips et al., 2000; Hou et al., 2005; Beatty, 1982b; Beatty, 1982a; Richer and Beatty, 1987; Einhäuser et al., 2008; Gilzenrat et al., 2010; Morad et al., 2000; Aston-Jones and Cohen, 2005; Murphy et al., 2011; Murphy et al., 2014). We supported and extended those findings by showing for the first time that the activity of subsets of LC+ neurons is related to subsequent changes in pupil diameter during stable, near fixation under several conditions: *i*) trial-by-trial associations between average pupil diameter and concurrent, tonic LC+ activation; *ii*) changes in spiking and LFP activity that occur just prior to pupil dilations; *iii*) trial-by-trial associations between the magnitude of pupil and LC+ neural responses evoked by unexpected presentations of the same auditory stimulus; and *iv*) evoked changes in pupil diameter via electrical microstimulation in the LC+. In general, we found that LC+ activity was higher just preceding pupil dilations versus constrictions, implying that the pupil changes do not cause changes in LC+ activation (e.g., via associated changes in visual input to the brain) but rather that both the pupil and LC+ may reflect underlying changes in arousal that can occur on fine timescales.

We also showed that relationships between neural activity and pupil diameter are not unique to the LC+ but instead can also be found for several other brain regions including the IC, SCi, ACC, and CGp. Substantial fractions of recorded units from each brain region exhibited spiking and LFP activity that was modulated in association with changes in pupil diameter, consistent with previous reports for numerous cortical regions in humans, non-human primates, and rodents performing various tasks (Vinck et al., 2015; Reimer et al., 2014; Ebitz and Platt, 2015; Eldar et al., 2013; McGinley et al., 2015). The effects in IC were particularly robust and, like for LC+ and SCi (Wang et al., 2012), could be elicited via electrical microstimulation. These widespread effects suggest that, at least during stable fixation and in the absence of complex task-related processing, neural activity throughout

many cortical and subcortical structures can be aligned in time with fluctuations in pupil diameter.

What mechanism can explain these phenomena? Constriction and dilation of the pupil is controlled by a balance of parasympathetic and sympathetic components, including inhibition of parasympathetic-controlled, tonic activation of the sphincter pupillae by the Edinger-Westphal nucleus and direct sympathetic activation of the dilator muscles (Loewenfeld, 1999). This balance is controlled by other circuits that give rise to pupil changes in response to changes in light, fixation, or other complex functions including arousal, orienting, and cognition (Andreassi, 2000). There are no known anatomical pathways that could subserve a direct influence of the LC+ on these autonomic circuits in primates (Nieuwenhuis et al., 2011). Instead, the relationship between LC+ activation and pupil diameter likely involves sources of common input to the two systems.

For external events that drive transient LC responses, this common driving force has been proposed to involve the paragigantocellularis nucleus (PGi) of the ventral medulla, which receives widespread cortical and subcortical inputs and projects to both Edinger-Westphal and the LC (Vogt et al., 2008; Breen et al., 1983; Nieuwenhuis et al., 2011). The PGi can mediate evoked, transient LC responses under at least some conditions (Hajós and Engberg, 1990; Ennis and Aston-Jones, 1988; Ennis et al., 1992; Chiang and Aston-Jones, 1993; Van Bockstaele et al., 1998). Thus, a circuit involving the PGi that co-modulates the LC and the sympathetic nervous system is consistent with our findings related to external event-(unexpected sound) related responses, which showed trial-by-trial relationships between neural- and pupil-response magnitude only for LC+. This circuit might also account for task-driven pupil changes previously reported to covary with activation of neurons in LC but not dopaminergic neurons in the substantia nigra, pars compacta, which is not known to receive substantial PGi inputs (Varazzani et al., 2015; Lee and Tepper, 2009; Bezard et al., 1997).

The PGi might also have contributed to our LC+ microstimulation effects. According to this idea, LC+ microstimulation causes direct, antidromic activation of PGi, which, in turn, affects the pupil in a consistent manner. The consistent LC+ effects might also reflect a relatively higher level of homogeneity in the functional properties of LC+ neurons around the sites of microstimulation, as compared to IC and SCi, although several recent studies have begun to challenge the long-held notion of LC as a functionally and anatomically uniform structure (Chandler et al., 2014; Schwarz et al., 2015).

Another, not mutually exclusive, possibility is a circuit that is centered on the SCi and the mesencephalic cuneiform nucleus (MCN) (Wang and Munoz, 2015). This pathway has been proposed to play a key role in changes in pupil diameter that are associated with certain aspects of cognitive processing including attention and orienting to salient stimuli (Wang and Munoz, 2015). Cholinergic modulation of these circuits also plays a role in attentional processing and might contribute to pupil effects, although such contributions have not yet been investigated directly (Yu and Dayan, 2005; Wang et al., 2006; Mysore and Knudsen, 2013). At the very least, these circuits involving the SCi likely contributed to our SCi microstimulation results. They might have also contributed to the sound-driven pupil changes, which likely reflected an abrupt change in arousal and attention. In principle, such

a contribution is possible even in the absence of consistent, trial-by-trial relationships between the sound-driven SCi and pupil responses, because those relationships measured via individual neurons are likely to be sensitive to the magnitude of correlated activity between individual SCi neurons (Shadlen et al., 1996), which has not yet been well characterized.

For our reported relationships between pupil diameter and neural activity in LC+ and elsewhere that occurred during sustained fixation and were not explicitly driven by external events, the underlying circuits are less clear. In humans, spontaneous fluctuations in pupil diameter are suppressed by opioids, leading to the suggestion that they are driven by fluctuating inputs to the Edinger-Westphal nucleus from opioid-sensitive neurons in the periacqueductal gray (Bokoch et al., 2015). These and other circuits, possibly including the PGi, SCi, MCN, and other brain areas that modulate autonomic control of the pupil during nominally steady-state conditions, may also contribute to co-activation of LC+ activity.

Regardless of the source of spontaneous, co-varying fluctuations in LC+ activation and pupil diameter during near fixation, one important consequence is the associated, timed release of NE throughout the brain. NE release can enhance both excitatory and inhibitory effects of incoming signals on targeted neurons, thus serving as a modulator of overall neural gain (Servan-Schreiber et al., 1990; Eldar et al., 2013; Aston-Jones and Cohen, 2005; Waterhouse et al., 1980; Segal and Bloom, 1976; Dillier et al., 1978). Such changes in gain, which also might involve astrocyte networks (Paukert et al., 2014) or other neuromodulatory and circuit mechanisms (Yu and Dayan, 2005; Lee and Dan, 2012; Salinas and Sejnowski, 2001; Haider and McCormick, 2009), would, in principle, affect coordinated activity throughout the brain in relation to the pupil changes that were co-modulated with the LC+ (Eldar et al., 2013; Aston-Jones and Cohen, 2005). Thus, according to this idea, pupil and LC+ are part of an arousal network that undergoes spontaneous fluctuations when an individual is in an attentive state but not necessarily performing an explicit task. These LC+ fluctuations, in turn, cause NE release that results in neural activity patterns throughout many parts of the brain that are coordinated with the pupil fluctuations, an idea that merits further study.

This neuromodulatory framework could, in principle and at least qualitatively, account for some of our results. In particular, we found that pupil-related changes in LC+ activity consistently preceded those found in IC and SCi in the same monkeys by many 10’s of ms. Accordingly, LC+-mediated NE release could have contributed to the changes in neural activity in these other brain regions (Aston-Jones and Cohen, 2005). However, such contributions do not exclude other network mechanisms. For example, the ACC both receives projections from and sends projections to LC+ and other brainstem nuclei, and CGp and ACC are heavily interconnected (Aston-Jones and Cohen, 2005; Porrino and Goldman-Rakic, 1982). These multiple pathways may help to explain the more variable and in some cases leading (Figs. 4–6) timing of pupil-related modulations of neuronal activity in cingulate cortex relative to LC+, IC, and SCi, which may in part reflect signals occurring first in cingulate and then transmitted to the LC+.

A combination of neuromodulatory and network effects may also account for our spectral results. Band-specific LFP power, which characterizes local oscillatory patterns, likely reflects network interactions (von Stein and Sarnthein, 2000; Kopell et al., 2000; Donner

and Siegel, 2011). In particular, local interactions are thought to underlie gamma-band enhancements, whereas the linkage of such local processing with integrative, cognitive processes is thought to enhance lower frequency bands. In our data, all three brainstem sites showed pupil-linked modulation in both frequency ranges. However, the LC+ had a distinctive relative abundance of higher versus lower frequency band modulations, suggesting pupil-linked changes in local processing there. Such local processing may include the integration of inputs into LC+ to generate spiking output, accompanied by release of NE elsewhere in the brain. This timed NE release, possibly in tandem with other neuromodulatory systems, may contribute to links between pupil fluctuations, network activity (or cortical states), and sensory, motor, and cognitive processing (Polack et al., 2013; Reimer et al., 2014; McGinley et al., 2015; Vinck et al., 2015; Sara and Bouret, 2012; Aston-Jones and Cohen, 2005; Briand et al., 2007). More work is needed to elucidate the specific, possibly neuromodulatory, mechanisms responsible for links between pupil changes and neural and behavioral phenomena that have been found for a much wider range of task conditions than we addressed in the present study.

EXPERIMENTAL PROCEDURES

Five adult male rhesus monkeys (Macaca mulatta) were used for this study. All training, surgery, and experimental procedures were performed in accordance with the National Institutes of Health's *Guide for the Care and Use of Laboratory Animals* and were approved by the University of Pennsylvania Institutional Animal Care and Use Committee.

Behavioral task

The monkeys performed a fixation task. All trials began with the presentation of a central fixation point. The monkey fixated for a variable period of time (1–5 s, uniformly distributed). The trial ended when the fixation point was turned off. The monkey was rewarded with a drop of water or Kool-Aid for maintaining fixation until the end of the trial. On about 25% of randomly chosen trials, a sound (1 kHz, 0.5 s) was played over a speaker in the experimental booth (beep trials) after 1–1.5 s of fixation. The monkey was required to maintain fixation through the presentation of the sound and until the fixation point was turned off.

Pupillometry

All measurements were made in a closed booth with the fixation point as the only source of luminance. To ensure reliable measurements of pupil diameter that were not influenced by changes in eye position (Hayes and Petrov, 2015), we included for analysis only periods of fixation that started at least 1 s after fixation onset and did not include any saccadic events, defined as changes in eye position with a minimum distance = 0.2 deg, minimum peak velocity = 0.08 deg/ms, minimum instantaneous velocity = 0.04 deg/ms, and minimum instantaneous acceleration = 0.005 deg/ms^2. Eye position was highly stable during these epochs (Mann-Whitney test for H_0: no difference in eye position at the beginning versus end of each fixation epoch, $p>0.05$ for 294/306 sessions across all monkeys). The fixation intervals included for analysis had a median [IQR] duration of 3108 [2539 3644] ms. Pupil diameter was measured monocularly in arbitrary units using a video-based eye-tracking

system (EyeLink 1000, SR Research Ltd.) sampled at 1000 Hz. Raw pupil measurements were z-scored for each session (for reference, an increase in pupil diameter of one standard deviation from the mean corresponded to a median [IQR] increase in pupil area of 21.3 [16.0–28.9]% across all sessions). To remove persistent effects of the changes in eye position and luminance that can result from fixation onset, the time-dependent, z-scored pupil trace from each trial was standardized by subtracting out the mean, across-trial pupil trace per session, aligned to fixation onset. Finally, these standardized traces were smoothed using a 151-ms-wide boxcar filter. Pupil slope was computed as the slope of a linear fit to a 151-ms-wide running window of the smoothed, standardized pupil-diameter measurements as a function of time within a trial. Pupil events were defined as maximum positive values (dilations) and negative values (constrictions) of the slope between sequential zero crossings of the slope separated by ≥75 ms. Microsaccades (Fig. 2E) were defined as changes in eye position with a minimum instantaneous velocity = 0.015 deg/ms and minimum duration = 6 ms.

Electrophysiology

Monkeys Oz and Ci were each implanted with a single recording cylinder that provided access to LC+, IC, and SCi. The detailed methodology for targeting and surgically implanting the recording cylinder and then targeting, identifying, and confirming recording sites in these three brain regions is described elsewhere for the exact sites used in this study (data for the two studies were collected in separate blocks in the same recording sessions) (Kalwani et al., 2014). Briefly, SCi units exhibited spatial tuning on a visually guided saccade task and could elicit saccades via electrical microstimulation (Robinson, 1972; Sparks and Nelson, 1987). IC units exhibited clear responses to auditory stimuli. LC+ units, which likely came from sites in either the LC or the adjacent, NE-containing subcoeruleus nucleus (Sharma et al., 2010; Paxinos et al., 2008; Kalwani et al., 2014), had relatively long action-potential waveforms, were sensitive to arousing external stimuli (e.g., door knocking), and decreased firing when the monkey was drowsy (e.g., eyelids drooped) (Aston-Jones et al., 1994; Bouret and Sara, 2004; Bouret and Richmond, 2009). These sites were verified using MRI and assessing the effects of systemic injection of clonidine on LC+ responses in both monkeys, and histology with electrolytic lesions and electrode-tract reconstruction in monkey Oz. Recording and microstimulation at these sites was conducted using custom-made electrodes (made from quartz-coated platinum-tungsten stock wire from Thomas Recording) and a Multi-channel Acquisition System (Plexon).

We targeted ACC and CGp on either the left side (monkeys Sp and Ch) or the right side (monkey At). ACC cylinders were placed at Horsley-Clark coordinates 33 mm AP, 8 mm L for monkey Sp and 43 mm AP, 8 mm L for monkey At. The CGp cylinder for monkey Sp was placed at 0 mm AP, 5 mm L, and tilted at an angle of 8.5 deg along the ML plane to point toward the midline. The CGp chamber for monkey Ch was placed at -5.3 AP, 12.2 mm L. For ACC recordings, we targeted the dorsal bank of the anterior cingulate sulcus (~4–6 mm below cortical surface). For CGp recordings, we targeted areas 31 and 23, in the posterior cingulate gyrus (~7–11 mm below cortical surface). Both brain regions were targeted using magnetic resonance imaging and custom software (Kalwani et al., 2009) as well as by listening for characteristic patterns of white and gray matter during recordings.

Recordings were conducted using either single-contact glass-coated tungsten electrodes (Alpha-Omega) or multicontact linear electrode arrays (V-probe, Plexon).

For each brain region, we recorded and analyzed data from all stable, well-isolated units that we encountered. Neural recordings were filtered between 100 Hz – 8 kHz for spikes and between 0.7 Hz – 170 Hz for LFPs. Spikes were sorted offline. Spectral analyses of the LFP were done using the Chronux toolkit (Bokil et al., 2010). LFP data were preprocessed using the "rmlinesc" function (Chronux) to remove 60 Hz line noise. Spectrograms were computed using a 0.5-s moving window with a 0.05-s step size, plus 19 tapers, resulting in spectral smoothing of +-20 Hz.

Electrical microstimulation in LC+, IC, or SCi consisted of biphasic (negative-positive) pulses, 0.3-ms long and delivered at 300 Hz via a Grass S-88 stimulator through a pair of constant-current stimulus isolation units (Grass PSIU6) that were linked together to generate the biphasic pulse. Microstimulation duration was 50, 100, or 400 ms. For LC+, microstimulation current was chosen in a range that did not evoke a visible startle response (10–30 μAmp). For IC, the same range was used. For SCi, the current was set at a value just below the threshold for evoking saccades (10–90 μAmp). We did not find any systematic differences in the probability, magnitude, or timing of evoked changes in pupil diameter using the different values of microstimulation duration or current amplitude, so the results are combined across all values of these parameters.

Data analysis

The magnitude of spontaneous and evoked changes in pupil diameter depends on baseline magnitude (Fig. 2D). Therefore, measured associations between the magnitude of spontaneous (Fig. 5) or evoked (Fig. 7) changes in pupil diameter with neural activity used partial correlations that accounted for effects of baseline pupil diameter on both variables.

ACKNOWLEDGEMENTS

We thank Long Ding, Takahiro Doi, and Merlin Larson for valuable comments and Jean Zweigle for expert animal care and training. The authors have no conflicts of interests to declare. Funded by NIH R21 MH-093904.

REFERENCES

Alnæs D, Sneve MH, Espeseth T, Endestad T, van de Pavert SH, Laeng B. Pupil size signals mental effort deployed during multiple object tracking and predicts brain activity in the dorsal attention network and the locus coeruleus. J Vis. 2014; 14:1, 20.

Alpern M, Mason GL, Jardinco RE. Vergence and accommodation. V. Pupil size changes associated with changes in accommodative vergence. Am J Ophthalmol. 1961; 52:762, 767. [PubMed: 13860699]

Andreassi, JL. Psychophysiology: Human behavior and physiological response. Lawrence Erlbaum Assoc.; Mahwah, NJ: 2000. Pupillary response and behavior; p. 218-233.

Aston-Jones G, Cohen JD. An integrative theory of locus coeruleus-norepinephrine function: adaptive gain and optimal performance. Annu Rev Neurosci. 2005; 28:403, 450. [PubMed: 16022602]

Aston-Jones G, Rajkowski J, Kubiak P, Alexinsky T. Locus coeruleus neurons in monkey are selectively activated by attended cues in a vigilance task. J Neurosci. 1994; 14:4467, 4480. [PubMed: 8027789]

Bari A, Aston-Jones G. Atomoxetine modulates spontaneous and sensory-evoked discharge of locus coeruleus noradrenergic neurons. Neuropharmacology. 2013; 64:53, 64. [PubMed: 22820275]

Beatty J. Phasic not tonic pupillary responses vary with auditory vigilance performance. Psychophysiology. 1982a; 19:167, 172. [PubMed: 7071295]

Beatty J. Task-evoked pupillary responses, processing load, and the structure of processing resources. Psychol Bull. 1982b; 91:276, 292. [PubMed: 7071262]

Bezard E, Boraud T, Bioulac B, Gross CE. Compensatory effects of glutamatergic inputs to the substantia nigra pars compacta in experimental parkinsonism. Neuroscience. 1997; 81:399, 404. [PubMed: 9300430]

Bokil H, Andrews P, Kulkarni JE, Mehta S, Mitra PP. Chronux: a platform for analyzing neural signals. J Neurosci Methods. 2010; 192:146, 151. [PubMed: 20637804]

Bokoch MP, Behrends M, Neice A, Larson MD. Fentanyl, an agonist at the mu opioid receptor, depresses pupillary unrest. Auton Neurosci. 2015; 189:68, 74. [PubMed: 25737234]

Bouret S, Richmond BJ. Relation of locus coeruleus neurons in monkeys to Pavlovian and operant behaviors. J Neurophysiol. 2009; 101:898, 911. [PubMed: 19091919]

Bouret S, Sara SJ. Reward expectation, orientation of attention and locus coeruleus-medial frontal cortex interplay during learning. Eur J Neurosci. 2004; 20:791, 802. [PubMed: 15255989]

Breen LA, Burde RM, Loewy AD. Brainstem connections to the Edinger-Westphal nucleus of the cat: a retrograde tracer study. Brain Res. 1983; 261:303, 306. [PubMed: 6831211]

Briand LA, Gritton H, Howe WM, Young DA, Sarter M. Modulators in concert for cognition: modulator interactions in the prefrontal cortex. Prog Neurobiol. 2007; 83:69, 91. [PubMed: 17681661]

Chandler DJ, Gao WJ, Waterhouse BD. Heterogeneous organization of the locus coeruleus projections to prefrontal and motor cortices. Proc Natl Acad Sci U S A. 2014; 111:6816, 6821. [PubMed: 24753596]

Chiang C, Aston-Jones G. Response of locus coeruleus neurons to footshock stimulation is mediated by neurons in the rostral ventral medulla. Neuroscience. 1993; 53:705, 715. [PubMed: 8487951]

Dillier N, Laszlo J, Müller B, Koella WP, Olpe HR. Activation of an inhibitory noradrenergic pathway projecting from the locus coeruleus to the cingulate cortex of the rat. Brain Res. 1978; 154:61, 68. [PubMed: 698822]

Donner TH, Siegel M. A framework for local cortical oscillation patterns. Trends Cogn Sci. 2011; 15:191, 199. [PubMed: 21481630]

Ebitz RB, Platt ML. Neuronal activity in primate dorsal anterior cingulate cortex signals task conflict and predicts adjustments in pupil-linked arousal. Neuron. 2015; 85:628, 640. [PubMed: 25654259]

Edwards SB, Ginsburgh CL, Henkel CK, Stein BE. Sources of subcortical projections to the superior colliculus in the cat. J Comp Neurol. 1979; 184:309, 329. [PubMed: 762286]

Einhäuser W, Koch C, Carter OL. Pupil dilation betrays the timing of decisions. Front Hum Neurosci. 2010; 4:1, 9. [PubMed: 20204154]

Einhäuser W, Stout J, Koch C, Carter O. Pupil dilation reflects perceptual selection and predicts subsequent stability in perceptual rivalry. Proc Natl Acad Sci U S A. 2008; 105:1704, 1709. [PubMed: 18250340]

Eldar E, Cohen JD, Niv Y. The effects of neural gain on attention and learning. Nat Neurosci. 2013; 16:1146, 1153. [PubMed: 23770566]

Ennis M, Aston-Jones G. Activation of locus coeruleus from nucleus paragigantocellularis: a new excitatory amino acid pathway in brain. J Neurosci. 1988; 8:3644, 3657. [PubMed: 3193175]

Ennis M, Aston-Jones G, Shiekhattar R. Activation of locus coeruleus neurons by nucleus paragigantocellularis or noxious sensory stimulation is mediated by intracoerulear excitatory amino acid neurotransmission. Brain Res. 1992; 598:185, 195. [PubMed: 1336704]

Foote SL, Bloom FE, Aston-Jones G. Nucleus locus ceruleus: new evidence of anatomical and physiological specificity. Physiol Rev. 1983; 63:844, 914. [PubMed: 6308694]

de Gee JW, Knapen T, Donner TH. Decision-related pupil dilation reflects upcoming choice and individual bias. Proc Natl Acad Sci U S A. 2014; 111:E618–E625. [PubMed: 24449874]

Gilzenrat MS, Nieuwenhuis S, Jepma M, Cohen JD. Pupil diameter tracks changes in control state predicted by the adaptive gain theory of locus coeruleus function. Cogn Affect Behav Neurosci. 2010; 10:252, 269. [PubMed: 20498349]

Granholm E, Steinhauer SR. Pupillometric measures of cognitive and emotional processes. Int J Psychophysiol. 2004; 52:1, 6. [PubMed: 15003368]

Haider B, McCormick DA. Rapid neocortical dynamics: cellular and network mechanisms. Neuron. 2009; 62:171, 189. [PubMed: 19409263]

Hajós M, Engberg G. A role of excitatory amino acids in the activation of locus coeruleus neurons following cutaneous thermal stimuli. Brain Res. 1990; 521:325, 328. [PubMed: 2169960]

Hayden BY, Heilbronner SR, Pearson JM, Platt ML. Surprise signals in anterior cingulate cortex: neuronal encoding of unsigned reward prediction errors driving adjustment in behavior. J Neurosci. 2011; 31:4178, 4187. [PubMed: 21411658]

Hayes TR, Petrov AA. Mapping and correcting the influence of gaze position on pupil size measurements. Behav Res Methods. 2015

Heilbronner SR, Haber SN. Frontal Cortical and Subcortical Projections Provide a Basis for Segmenting the Cingulum Bundle: Implications for Neuroimaging and Psychiatric Disorders. J Neurosci. 2014; 34:10041, 10054. [PubMed: 25057206]

Hormigo S, Horta Júnior J.d.e. .A. Gómez-Nieto R, López DE. The selective neurotoxin DSP-4 impairs the noradrenergic projections from the locus coeruleus to the inferior colliculus in rats. Front Neural Circuits. 2012; 6:1, 14. [PubMed: 22291618]

Hou RH, Freeman C, Langley RW, Szabadi E, Bradshaw CM. Does modafinil activate the locus coeruleus in man? Comparison of modafinil and clonidine on arousal and autonomic functions in human volunteers. Psychopharmacology (Berl). 2005; 181:537, 549. [PubMed: 15983798]

Hunter JD, Milton JG, Lüdtke H, Wilhelm B, Wilhelm H. Spontaneous fluctuations in pupil size are not triggered by lens accommodation. Vision Res. 2000; 40:567, 573. [PubMed: 10820614]

Jepma M, Nieuwenhuis S. Pupil diameter predicts changes in the exploration-exploitation trade-off: evidence for the adaptive gain theory. J Cogn Neurosci. 2011; 23:1587, 1596. [PubMed: 20666595]

Kahneman D, Beatty J. Pupil diameter and load on memory. Science. 1966; 154:1583, 1585. [PubMed: 5924930]

Kalwani RM, Bloy L, Elliott MA, Gold JI. A method for localizing microelectrode trajectories in the macaque brain using MRI. J Neurosci Methods. 2009; 176:104–11. [PubMed: 18831988]

Kalwani RM, Joshi S, Gold JI. Phasic activation of individual neurons in the locus ceruleus/subceruleus complex of monkeys reflects rewarded decisions to go but not stop. J Neurosci. 2014; 34:13656, 13669. [PubMed: 25297093]

Klepper A, Herbert H. Distribution and origin of noradrenergic and serotonergic fibers in the cochlear nucleus and inferior colliculus of the rat. Brain Res. 1991; 557:190, 201. [PubMed: 1747753]

Kopell N, Ermentrout GB, Whittington MA, Traub RD. Gamma rhythms and beta rhythms have different synchronization properties. Proc Natl Acad Sci U S A. 2000; 97:1867, 1872. [PubMed: 10677548]

Krekelberg B. Microsaccades. Curr Biol. 2011; 21:R416. [PubMed: 21640896]

Krugman HE. Some applications of pupil measurement. Journal of Marketing Research. 1964; 1:15, 19.

Lavín C, San Martín R, Rosales Jubal E. Pupil dilation signals uncertainty and surprise in a learning gambling task. Front Behav Neurosci. 2014; 7:218. [PubMed: 24427126]

Lee CR, Tepper JM. Basal ganglia control of substantia nigra dopaminergic neurons. J Neural Transm. 2009; (Suppl):71–90. [PubMed: 18972063]

Lee SH, Dan Y. Neuromodulation of brain states. Neuron. 2012; 76:209, 222. [PubMed: 23040816]

Levitt P, Moore RY. Noradrenaline neuron innervation of the neocortex in the rat. Brain Res. 1978; 139:219, 231. [PubMed: 624057]

Loewenfeld, IE. The pupil: anatomy, physiology, and clinical applications. Butterworth and Heinemann; Boston, MA: 1999.

Loewenfeld IE, Newsome DA. Iris mechanics. I. Influence of pupil size on dynamics of pupillary movements. Am J Ophthalmol. 1971; 71:347, 362. [PubMed: 5100474]

Martinez-Conde S, Otero-Millan J, Macknik SL. The impact of microsaccades on vision: towards a unified theory of saccadic function. Nat Rev Neurosci. 2013; 14:83, 96. [PubMed: 23329159]

McGinley MJ, David SV, McCormick DA. Cortical Membrane Potential Signature of Optimal States for Sensory Signal Detection. Neuron. 2015; 87:179, 192. [PubMed: 26074005]

Morad Y, Lemberg H, Yofe N, Dagan Y. Pupillography as an objective indicator of fatigue. Curr Eye Res. 2000; 21:535, 542. [PubMed: 11035533]

Murphy PR, O'Connell RG, O'Sullivan M, Robertson IH, Balsters JH. Pupil diameter covaries with BOLD activity in human locus coeruleus. Hum Brain Mapp. 2014; 35:4140, 4154. [PubMed: 24510607]

Murphy PR, Robertson IH, Balsters JH, O'Connell RG. Pupillometry and P3 index the locus coeruleus-noradrenergic arousal function in humans. Psychophysiology. 2011; 48:1532, 1543. [PubMed: 21762458]

Mysore SP, Knudsen EI. A shared inhibitory circuit for both exogenous and endogenous control of stimulus selection. Nat Neurosci. 2013; 16:473, 478. [PubMed: 23475112]

Nassar MR, Rumsey KM, Wilson RC, Parikh K, Heasly B, Gold JI. Rational regulation of learning dynamics by pupil-linked arousal systems. Nat Neurosci. 2012; 15:1040, 1046. [PubMed: 22660479]

Nieuwenhuis S, De Geus EJ, Aston-Jones G. The anatomical and functional relationship between the P3 and autonomic components of the orienting response. Psychophysiology. 2011; 48:162, 175. [PubMed: 20557480]

Paukert M, Agarwal A, Cha J, Doze VA, Kang JU, Bergles DE. Norepinephrine controls astroglial responsiveness to local circuit activity. Neuron. 2014; 82:1263, 1270. [PubMed: 24945771]

Paxinos G, Huang X-F, Petrides M, Toga A. The Rhesus monkey brain: in stereotaxic coordinates. 2008

Phillips MA, Szabadi E, Bradshaw CM. Comparison of the effects of clonidine and yohimbine on pupillary diameter at different illumination levels. Br J Clin Pharmacol. 2000; 50:65, 68. [PubMed: 10886121]

Polack PO, Friedman J, Golshani P. Cellular mechanisms of brain state-dependent gain modulation in visual cortex. Nat Neurosci. 2013; 16:1331, 1339. [PubMed: 23872595]

Porrino LJ, Goldman-Rakic PS. Brainstem innervation of prefrontal and anterior cingulate cortex in the rhesus monkey revealed by retrograde transport of HRP. J Comp Neurol. 1982; 205:63, 76. [PubMed: 6121826]

Preuschoff K, 't Hart BM, Einhäuser W. Pupil Dilation Signals Surprise: Evidence for Noradrenaline's Role in Decision Making. Front Neurosci. 2011; 5:115. [PubMed: 21994487]

Reimer J, Froudarakis E, Cadwell CR, Yatsenko D, Denfield GH, Tolias AS. Pupil Fluctuations Track Fast Switching of Cortical States during Quiet Wakefulness. Neuron. 2014; 84:355, 362. [PubMed: 25374359]

Richer F, Beatty J. Contrasting effects of response uncertainty on the task-evoked pupillary response and reaction time. Psychophysiology. 1987; 24:258, 262. [PubMed: 3602280]

Robinson DA. Eye movements evoked by collicular stimulation in the alert monkey. Vision Res. 1972; 12:1795, 1808. [PubMed: 4627952]

Salinas E, Sejnowski TJ. Gain modulation in the central nervous system: where behavior, neurophysiology, and computation meet. Neuroscientist. 2001; 7:430, 440. [PubMed: 11597102]

Sara SJ, Bouret S. Orienting and reorienting: the locus coeruleus mediates cognition through arousal. Neuron. 2012; 76:130, 141. [PubMed: 23040811]

Schmidt, HS.; Fortin, LD. Electronic pupillography in disorders of arousal. In: Fortin, LD.; Schmidt, HS.; Guilleminault, editors. Sleeping and waking disorders: Indication and technique. Addison-Wesley; Menlo Park, CA: 1982. p. 127-143.

Schwarz LA, Miyamichi K, Gao XJ, Beier KT, Weissbourd B, DeLoach KE, Ren J, Ibanes S, Malenka RC, Kremer EJ, Luo L. Viral-genetic tracing of the input-output organization of a central noradrenaline circuit. Nature. 2015; 524:88, 92. [PubMed: 26131933]

Segal M, Bloom FE. The action of norepinephrine in the rat hippocampus. III. Hippocampal cellular responses to locus coeruleus stimulation in the awake rat. Brain Res. 1976; 107:499, 511. [PubMed: 178410]

Servan-Schreiber D, Printz H, Cohen JD. A network model of catecholamine effects: gain, signal-to-noise ratio, and behavior. Science. 1990; 249:892, 895. [PubMed: 2392679]

Shadlen MN, Britten KH, Newsome WT, Movshon JA. A computational analysis of the relationship between neuronal and behavioral responses to visual motion. J Neurosci. 1996; 16:1486, 1510. [PubMed: 8778300]

Sharma Y, Xu T, Graf WM, Fobbs A, Sherwood CC, Hof PR, Allman JM, Manaye KF. Comparative anatomy of the locus coeruleus in humans and nonhuman primates. J Comp Neurol. 2010; 518:963, 971. [PubMed: 20127761]

Sparks DL, Nelson JS. Sensory and motor maps in the mammalian superior colliculus. Trends Neurosci. 1987; 10:312, 317.

Stanten SF, Stark L. A statistical analysis of pupil noise. IEEE Trans Biomed Eng. 1966; 13:140, 152. [PubMed: 5946423]

Stark LR, Atchison DA. Pupil size, mean accommodation response and the fluctuations of accommodation. Ophthalmic Physiol Opt. 1997; 17:316, 323. [PubMed: 9390376]

Takeuchi T, Puntous T, Tuladhar A, Yoshimoto S, Shirama A. Estimation of mental effort in learning visual search by measuring pupil response. PLoS One. 2011; 6:e21973. [PubMed: 21760936]

Van Bockstaele EJ, Colago EE, Aicher S. Light and electron microscopic evidence for topographic and monosynaptic projections from neurons in the ventral medulla to noradrenergic dendrites in the rat locus coeruleus. Brain Res. 1998; 784:123, 138. [PubMed: 9518578]

Varazzani C, San-Galli A, Gilardeau S, Bouret S. Noradrenaline and dopamine neurons in the reward/effort trade-off: a direct electrophysiological comparison in behaving monkeys. J Neurosci. 2015; 35:7866, 7877. [PubMed: 25995472]

Vinck M, Batista-Brito R, Knoblich U, Cardin JA. Arousal and locomotion make distinct contributions to cortical activity patterns and visual encoding. Neuron. 2015; 86:740, 754. [PubMed: 25892300]

Vogt BA, Hof PR, Friedman DP, Sikes RW, Vogt LJ. Norepinephrinergic afferents and cytology of the macaque monkey midline, mediodorsal, and intralaminar thalamic nuclei. Brain Struct Funct. 2008; 212:465, 479. [PubMed: 18317800]

von Stein A, Sarnthein J. Different frequencies for different scales of cortical integration: from local gamma to long range alpha/theta synchronization. Int J Psychophysiol. 2000; 38:301, 313. [PubMed: 11102669]

Wang CA, Munoz DP. A circuit for pupil orienting responses: implications for cognitive modulation of pupil size. Curr Opin Neurobiol. 2015; 33:134, 140. [PubMed: 25863645]

Wang CA, Boehnke SE, Itti L, Munoz DP. Transient pupil response is modulated by contrast-based saliency. J Neurosci. 2014; 34:408, 417. [PubMed: 24403141]

Wang CA, Boehnke SE, White BJ, Munoz DP. Microstimulation of the monkey superior colliculus induces pupil dilation without evoking saccades. J Neurosci. 2012; 32:3629, 3636. [PubMed: 22423086]

Wang Y, Luksch H, Brecha NC, Karten HJ. Columnar projections from the cholinergic nucleus isthmi to the optic tectum in chicks (Gallus gallus): a possible substrate for synchronizing tectal channels. J Comp Neurol. 2006; 494:7, 35. [PubMed: 16304683]

Warga M, Lüdtke H, Wilhelm H, Wilhelm B. How do spontaneous pupillary oscillations in light relate to light intensity? Vision Res. 2009; 49:295, 300. [PubMed: 18851988]

Waterhouse BD, Moises HC, Woodward DJ. Noradrenergic modulation of somatosensory cortical neuronal responses to iontophoretically applied putative neurotransmitters. Exp Neurol. 1980; 69:30, 49. [PubMed: 7389849]

Yu AJ, Dayan P. Uncertainty, neuromodulation, and attention. Neuron. 2005; 46:681, 692. [PubMed: 15944135]

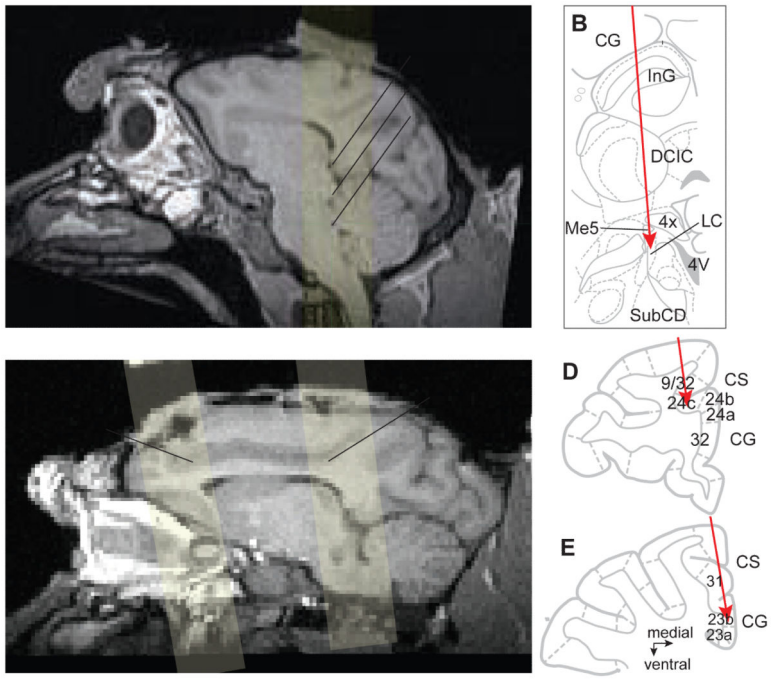

Figure 1.

Recording site locations. (A) Approximately sagittal MRI section for monkey Ci showing estimated recording site locations in SCi, IC, and LC+, along with the approximate depth from the cortical surface along the electrode tract. (B) Schematic of a coronal section of the macaque brain showing structures typically encountered along our electrode tracts (adapted from (Paxinos et al., 2008), Plate 90, Interaural 0.3, bregma 21.60; see also (Kalwani et al., 2014), Fig. 3). (C) Approximately sagittal MRI section for monkey Sp showing estimated recording sites in ACC and CGp, along with the approximate depth from the cortical surface along the electrode tract. (D, E) Schematic of a coronal section of the macaque brain showing structures typically encountered along our electrode tracts to ACC (D; adapted from (Paxinos et al., 2008), Plate 16, Interaural 33.60, bregma 11.70) or CGp (E; adapted from (Paxinos et al., 2008), Plate 89, Interaural 0.75, bregma -21.15). Lightly shaded yellow regions in (A) and (C) correspond to the three-dimensional projections of the recording cylinder (Kalwani et al., 2009). Arrows in (B), (D), and (E) show approximate electrode tracts. CG: cingulate gyrus; CS: cingulate sulcus; DCIC: dorsal complex of the IC; InG: intermediate gray of the SC; me5: mesencephalic 5 tract; subCD: dorsal subcoeruleus; 4v: fourth ventricle; 4x: trochlear decussation; 9/32, 24c: ACC (dorsal); 32, 24a, 24b: ACC (ventral); 23a, 23b, 31: CGp.

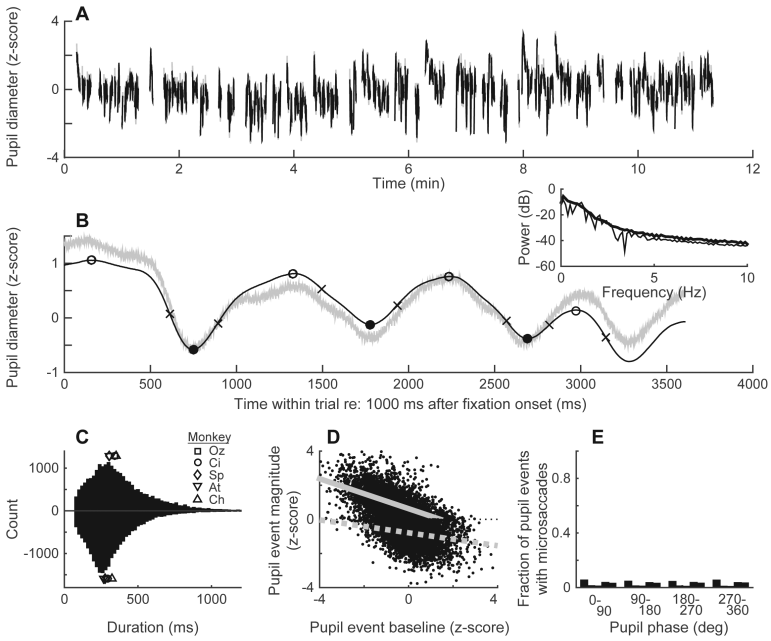

Figure 2.

Measuring pupil diameter. (A) Pupil diameter measured during one recording session (Monkey Oz). Only stable fixation epochs used for further analyses are shown; thus, data breaks represent unstable fixations and inter-trial intervals. (B) Single-trial raw (gray) and smoothed and standardized (black) pupil trace during stable fixation. Open and closed circles indicate local maxima and minima, respectively, which define pupil "events." Crosses indicate the peak slope of the pupil signal between extrema. Inset shows pupil power spectrum (thin line is the example trial, thick line is trial mean for this session). (C) Distribution of pupil event durations for all monkeys and all sessions. Dilation times (intervals between each local minimum and the subsequent maximum) are shown above the x-axis, whereas constriction times (intervals between each local maximum and the subsequent minimum) are shown below it. Median values for each of the 5 monkeys are shown as different (overlapping) symbols, as indicated. (D) Per-cycle pupil event baseline versus fluctuation magnitude, measured for one representative monkey. Gray lines show linear regressions for dilations (solid) and constrictions (dashed). (E) Proportion of pupil events with microsaccades, plotted as a function of the phase of the pupil event in which it occurred (five bars per bin represent the five monkeys, ordered as in the legend in panel C). For all five monkeys, the distributions were uniform with respect to phase (Rayleigh test, $p>0.05$).

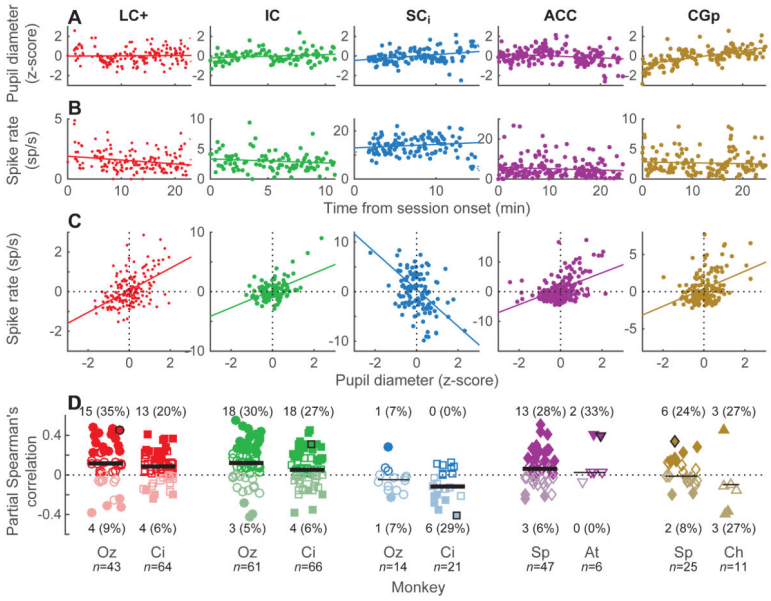

Figure 3.

Trial-by-trial associations between mean pupil diameter and spike rate for each brain region, as indicated (columns). (A–C) Example sessions. Per-trial mean pupil diameter (A) and spike rate (B) are each plotted as a function of the time of the beginning of stable fixation in the given trial, with respect to the beginning of the session. Lines are linear fits. Panel C shows residuals to these fits. The line is a linear fit to the paired residuals, representing the partial correlation between pupil diameter and spike rate, accounting for linear drifts of each variable as a function of time within the session. (D) Distributions of Spearman's partial correlations (ρ) between trial-by-trial pupil diameter and spike rate, accounting for time within the session, for each session from each monkey and each brain region, as indicated. Darker/lighter symbols indicate $\rho>0/\rho<0$. Filled symbols indicate H_0: $\rho=0$, $p<0.05$. Counts (percentages) of significant positive/negative effects are shown for each monkey (per-monkey percentages for positive or negative effects were indistinguishable between LC+ and IC but were different for SCi, including fewer positive effects for both monkeys and more negative effects for monkey Ci; chi-squared test, $p<0.05$). Black symbols indicate the example sessions above. Scatter along the abscissa is arbitrary, for readability. Horizontal lines are medians; thick lines indicate H_0: median=0, Wilcoxon rank-sum test $p<0.05$.

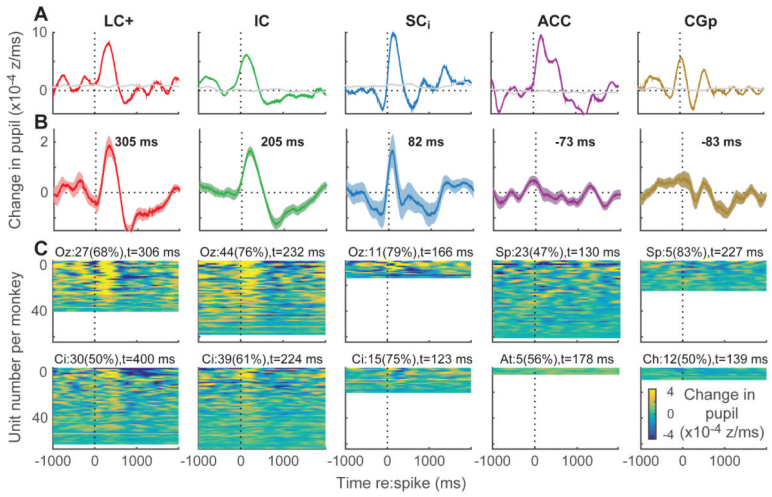

Figure 4.

Spike-triggered changes in pupil diameter for each brain region, as indicated (columns). (A) Example units. Colored lines are mean values computed from all spikes recorded during stable fixation in the given session. Gray lines are values computed after shuffling pupil diameter relative to spiking activity on a trial-by-trial basis. (B) Mean±sem spike-triggered changes in pupil diameter computed from the mean, real– shuffled curves computed for each recorded unit from the two monkeys. The time of the maximum value is shown; bold indicates H_0: the value at that time=0, $p<0.05$ bootstrapped from the mean±sem values computed per unit for the given time bin. (C) Mean spike-triggered changes in pupil diameter for all recorded single units, sorted by modulation depth per monkey (top rows show units with the biggest difference between the minimum and maximum values). Text indicates the count (percentage) of sites for each monkey with a reliable peak (defined as ≥75 consecutive bins with at least one bin between 100 ms before and 700 ms after the spike for which real–shuffled was significantly >0, Mann-Whitney $p<0.05$) and the median time of the reliable peaks. Per-monkey percentages were indistinguishable between LC+, IC, and SCi (chi-squared test, $p\geq0.05$). All analyses used 250-ms time bins stepped in 10-ms intervals.

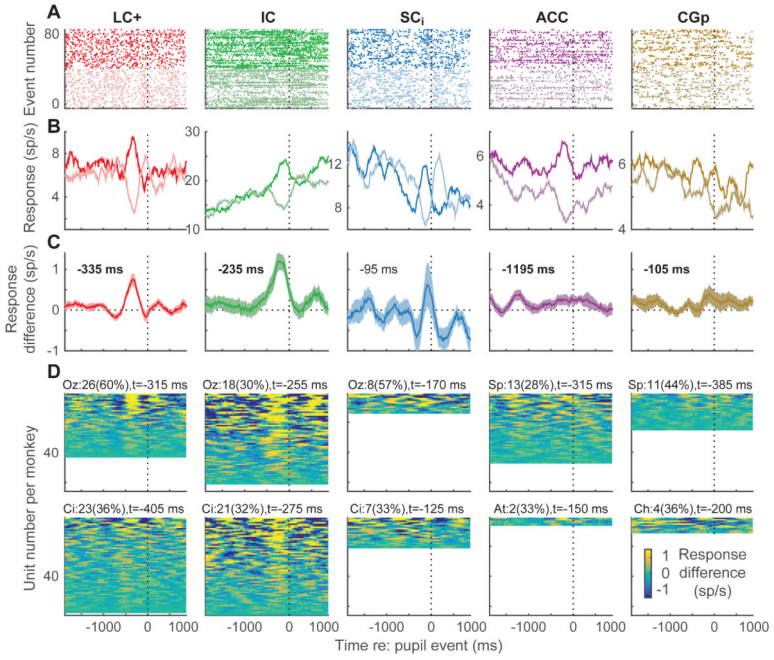

Figure 5.

Spike PETHs aligned to pupil events for each brain region, as indicated (columns). (A, B) Example units. Light/dark lines show rasters (A, showing 40 randomly selected trials for each condition for presentation clarity) and PETHs (B) for large dilation/constriction events (upper/lower 25th percentile slopes; see Fig. 2B), aligned to the time of the event. (C) Mean ±sem difference in dilation-versus constriction-aligned PETHs computed for each recorded unit from the two monkeys. The time of the maximum value is shown in each panel; bold indicates H_0: the value at that time=0, $p<0.05$ bootstrapped from the mean±sem values computed per unit for the given time bin. (D) Mean difference in dilation-versus constriction-aligned PETHs computed for all recorded single units, sorted by modulation depth per monkey (top rows show units with the biggest difference between the maximum and minimum values). Text indicates the count (percentage) of sites for each monkey with a reliable peak (defined as ≥75 consecutive bins with at least one bin between 100 ms before and 700 ms after the spike for which real–shuffled was significantly >0, Mann-Whitney $p<0.05$) and the median time of the reliable peaks. Per-monkey percentages were indistinguishable between LC+, IC, and SCi (chi-squared test, $p\geq0.05$) except for Oz, LC vs. IC. All analyses used 250-ms time bins stepped in 10-ms intervals.

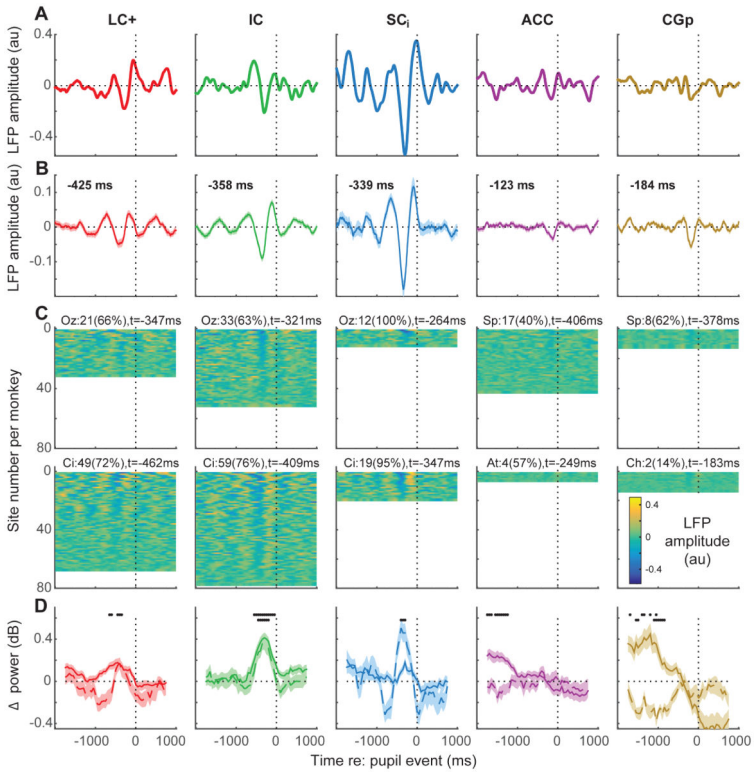

Figure 6.

Pupil-related differences in LFP time course and power spectrum for each brain region, as indicated (columns). (A) Differences in time-series LFPs aligned to large pupil events (dilate–constrict) for example recording sites. (B) Mean±sem differences in time-series LFPs aligned to large pupil events computed for each recorded site from the two monkeys. The time of the minimum value from the mean curve is shown; bold indicates H_0: the value at that time=0, $p<0.05$ bootstrapped from the mean±sem values computed per site for the given time bin. (C) Mean differences in time-series LFPs aligned to large pupil events computed for all recording sites, sorted by modulation depth per monkey (top rows show units with the biggest difference between dilation- and constriction-linked values). Text indicates the count (percentage) of sites for each monkey with a reliable trough (defined as ≥75 consecutive bins with at least one bin in the 1000 ms preceding the pupil event with a value that was significantly <0, Wilcoxon rank-sum test $p<0.05$) and the median time of the reliable troughs. (D) Difference (dilate–constrict) in LFP power spectra aligned to pupil events for low (<30Hz, dashed line) and gamma (30–100Hz) frequency bands. Black dots indicate H_0: binned value=0, Mann-Whitney $p<0.05$ corrected for multiple comparisons (upper row: gamma band; lower row: low-frequency band). All analyses used 500-ms time bins stepped in 50-ms intervals.

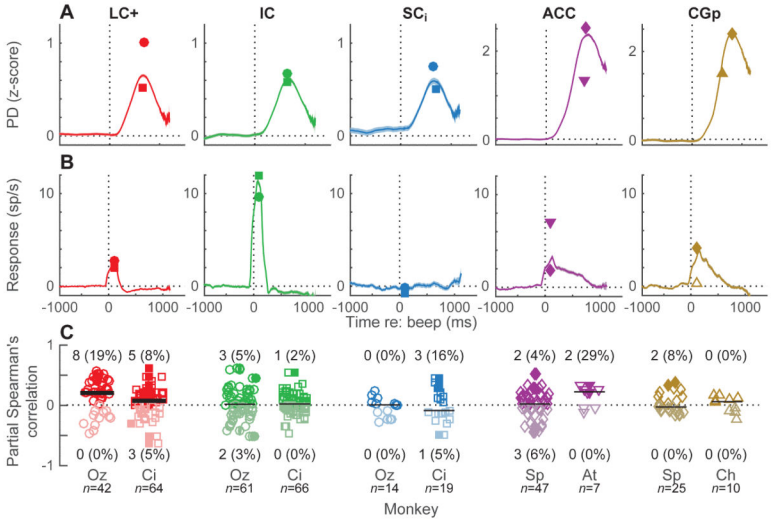

Figure 7.

Responses to startling events for each brain region, as indicated (columns). (A) Transient pupil dilations evoked by unexpected auditory events (“beeps”). (B) Spiking responses to unexpected auditory events, measured in 200-ms time bins stepped in 10-ms intervals. In (A) and (B), lines/ribbons are mean/SEM across all beep trials from both monkeys. Symbols are maximum values per monkey. (C) Population summary. Spearman’s partial correlation, ρ, between spiking (spike rate 0–200 ms following beep onset minus baseline spike rate measured during fixation prior to beep onset) and pupil (maximum change in pupil diameter 0–800 ms following beep onset) responses, accounting for the effects of baseline pupil diameter on both variables. Darker/lighter symbols indicate $\rho>0/\rho<0$. Filled symbols indicate H_0: $\rho=0$, $p<0.05$. Counts (percentages) of significant positive/negative effects are shown for each monkey (for monkey Oz, the percentages for positive effects were significantly different for LC vs. IC or SCi; chi-squared test, $p<0.05$). Scatter along the abscissa is arbitrary, for readability. Horizontal lines are medians; thick line indicates H_0: median=0, Wilcoxon rank-sum test $p<0.05$.

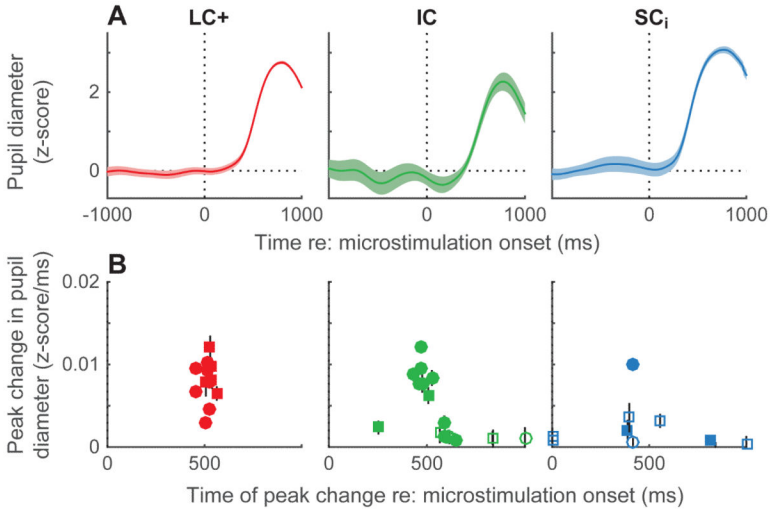

Figure 8.

Effects of electrical microstimulation in LC+, IC, and SCi (columns) on pupil diameter. (A) Pupil diameter aligned to the time of microstimulation onset. Lines and ribbons are mean ±SEM across all microstimulation trials from all sessions. (B) Summary of microstimulation effects. Symbols and error bars are mean±SEM peak change in pupil diameter <800 ms following microstimulation onset from individual trials in a given session, plotted as a function of the time of the peak. Closed symbols indicate H_0: peak change=0, Wilcoxon rank-sum test $p<0.05$.